ON COMBINED EFFECT OF THERMAL RADIATION AND VISCOUS DISSIPATION IN HYDROMAGNETIC MICROPOLAR FLUID FLOW BETWEEN TWO STRETCHABLE DISKS

Kashif ALI, Shahzad AHMAD[1] , Muhammad ASHRAF

Centre for Advanced Studies in Pure and Applied Mathematics, Bahauddin Zakariya University, Multan, Pakistan

In this paper, we investigate numerically the flow and heat transfer characteristics of a viscous incompressible electrically conducting micropolar fluid between two infinite uniformly stretching disks, taking the radiation and viscous dissipation effects into consideration. The transformed self similar coupled ODEs are solved using quasi linearization method. The study may be beneficial in flow and thermal control of polymeric processing.

Key words: *Magnetohydrodynamics (MHD); Micropolar fluid; Stretchable disks; Radiation; Viscous dissipation; Nusselt number*

1. Introduction

In the recent years, the investigation of flow over a stretching surface has attracted the attention of research community due to its significant applications in different industries such as extrusion paper production, extrusion of polymers sheet, metal and plastic industries [1-3]. The problem of fluid flow between parallel disks is also important due to its applications in many technological and engineering processes. These applications include semiconductor-manufacturing processes with rotating wafers, magnetic storage devices, gas turbine engines, hydrodynamical machines and apparatus, crystal growth processes, rotating machinery, biomechanics, geothermal, geophysical, heat and mass exchanges, computer storage devices, viscometry, lubrication, oceanography radial diffusers etc. Singh *et al* [4] analyzed the inward flow between two stationery parallel disks and find out the solution by experimental as well as numerical methods. Fang *et al* [5] determined exact solution of the Navier Stokes equations analytically to study the MHD viscous flow under slip conditions over a permeable stretching surface. On the other hand, Volkan [6] used the analytic approach to find an approximate solution for the problem of flow between two disks rotating about distinct axes at different speeds. Ahmad *et al* [7] used a similarity transformation to investigate the boundary layer flow of an electrically conducting fluid over a stretching plate. Yoon *et al* [8] numerically investigated the flow and heat transfer near an infinite disk with surface roughness, which rotates steadily about the longitudinal axis. An analytical solution of axis- symmetric flow between two infinite stretching disks was presented by Robert *et al* [9]. Fang and Zhang [10] gave the exact solution for the axis-symmetric flow between two stretchable infinite disks. Munawar *et al* [11] employed the Optimal HAM to study the flow of an incompressible viscous fluid between two continuously stretching coaxial disks. On the other hand, flow of an electrically conducting fluid on a stretching rotating disk was studied by Turkyilmazoglu [12] & [13] by means of similarity transformations. Attia [14] analyzed the problem of steady flow of an incompressible viscous fluid over an infinite rotating disk through porous medium with heat transfer. Xinhui *et al* [15] studied the asymmetric flow and heat transfer of viscous fluid between contracting/expanding rotating disks by using homotopy analysis method.

It has been noticed that the Newtonian model is not appropriate to completely describe some modern engineering and industrial processes which involve fluids, possessing an internal structure. Fluids having polymeric additives display a significant reduction of shear stress and polymeric concentration, as

E-mail address for correspondence: shahzadahmadbzu@gmail.com)

predicted experimentally by Hoyt and Fabula [16]. The deformation of such materials has been well explained by the theory of micropolar fluids introduced by Eringen [17]. The flow of colloidal solutions, liquid crystals, polymeric fluids & blood are some of the examples where the micropolar fluid model may be employed. For further details regarding the applications of the micropolar fluid model, please see Rashidi *et al* [18], and Hayat and Nawaz [19]. Micropolar fluid is an active area of research in which different aspects of the problems are being studied, in every possible detail. The problem of steady axisymmetric flow and heat transfer in an incompressible micropolar fluid between two porous disks was studied by Takhar *et al* [20] whereas the flow over an enclosed rotating disk was analyzed by Takhar *et al* [21]. Similarly, Magnetohydrodynamics(MHD) has attracted the research community due to its novel industrial applications. Excellent literature survey on the subject may be found in Rashidi and Keimanesh [22], Rashidi *et al* [23] and Rashidi and Erfani [24].

The above mentioned researchers did not take the effects of viscous dissipation & thermal radiation in their investigations. Therefore, the aim of the present study is to investigate MHD steady viscous incompressible electrically conducting micropolar fluid flow and heat transfer between two stretching disks in the presence of a transverse magnetic field with radiation and viscous dissipation effects.

2. Problem formulation

We consider steady laminar viscous incompressible flow and heat transfer of an electrically conducting micropolar fluid between two stretchable infinite disks, located at $z=-h$ & $z=h$ as shown in Fig. 2. A uniform transverse magnetic field $\underline{B}$ is applied perpendicularly at the disks. The geometry of the problem suggests that the cylindrical polar coordinate system is most suitable for the study. Both the disks are stretching uniformly with the velocity proportional to the r coordinate. The magnetic Reynolds number is assumed to be small and hence the induced magnetic field can be neglected as compared to the imposed magnetic field (Shercliff [25]). We assume that there is no applied polarization voltage, so the electric field is zero.

Following (Hayat *et al* [26]), the governing momentum equations, in vector form, for the present problem are:

$$\nabla.(\underline{V})=0 \tag{1}$$

$$(\mu+\kappa)\nabla^2\underline{V}+\kappa\nabla\times\underline{\upsilon}-\nabla p+\underline{J}\times\underline{B}=\rho\dot{\underline{V}} \tag{2}$$

$$(\alpha+\beta+\gamma)\nabla(\nabla\cdot\underline{\upsilon})-\gamma(\nabla\times\nabla\times\underline{\upsilon})+\kappa\nabla\times\underline{V}-2\kappa\underline{\upsilon}=\rho j\dot{\underline{\upsilon}} \tag{3}$$

$$\underline{J}=\sigma_e(\underline{V}\times\underline{B}) \tag{4}$$

where $\underline{V}$ is the velocity field, p is the pressure, μ is the dynamic viscosity of the fluid, κ is the vortex viscosity , j is the micro-inertia per unit mass, $\underline{\upsilon}$ is the micro-rotation vector, ρ is the fluid density, μ and k are the viscosity coefficients, $\underline{J}$ the current density, $\underline{B}$ the total magnetic field so that $\underline{B}=\underline{B}_0+\underline{b}$, $\underline{b}$ the induced magnetic field, σ_e the electrical conductivity of the fluid and α,β and γ are the gyroviscosity coefficients. Furthermore μ,κ,α,β and γ satisfy the following constraints:

$2\mu+\kappa\geq 0,\kappa\geq 0,3\alpha+\beta+\gamma\geq 0,\gamma\geq|\beta|$.

The velocity and micro-rotion fields for the problem are

$$\underline{V}=(u_r,0,u_z)\text{ and }\underline{\upsilon}=(0,\upsilon_2,0), \tag{5}$$

where $u_r=u_r(r,z),u_z=u_z(r,z)$ and $\upsilon_2=\upsilon_2(r,z)$.

The above set of equations may be written in component form as:

$$\frac{u_r}{r}+\frac{\partial u_r}{\partial r}+\frac{1}{h}\frac{\partial u_z}{\partial \eta}=0, \tag{6}$$

$$\rho(u_r\frac{\partial u_r}{\partial r}+\frac{u_z}{h}\frac{\partial u_r}{\partial \eta})=-\frac{\partial p}{\partial r}-\frac{\kappa}{h}\frac{\partial \upsilon_2}{\partial \eta}+(\mu+\kappa)(\frac{\partial^2 u_r}{\partial r^2}+\frac{1}{r}\frac{\partial u_r}{\partial r}-\frac{u_r}{r^2}+\frac{1}{h^2}\frac{\partial^2 u_r}{\partial \eta^2})-\sigma_e {B_0}^2 u_r, \tag{7}$$

$$\rho(u_r\frac{\partial u_z}{\partial r}+\frac{u_z}{h}\frac{\partial u_z}{\partial \eta})=-\frac{1}{h}\frac{\partial p}{\partial \eta}+\kappa(\frac{\partial \upsilon_2}{\partial r}+\frac{\upsilon_2}{r})+(\mu+\kappa)(\frac{\partial^2 u_z}{\partial r^2}+\frac{1}{r}\frac{\partial u_z}{\partial r}+\frac{1}{h^2}\frac{\partial^2 u_z}{\partial \eta^2}), \tag{8}$$

$$\rho j(u_r\frac{\partial \upsilon_2}{\partial r}+\frac{u_z}{h}\frac{\partial \upsilon_2}{\partial \eta})=\kappa(\frac{1}{h}\frac{\partial u_r}{\partial \eta}-\frac{\partial u_z}{\partial r})-2\kappa\upsilon_2+\gamma(\frac{\partial^2 \upsilon_2}{\partial r^2}-\frac{\upsilon_2}{r^2}+\frac{1}{r}\frac{\partial \upsilon_2}{\partial r}+\frac{1}{h^2}\frac{\partial^2 \upsilon_2}{\partial \eta^2}), \tag{9}$$

where η is the similarity variable, B_0 is the strength of the magnetic field. Including the thermal radiation & viscous dissipation effects, the energy equation for the problem of flow between two stretching disks can be written as

$$\rho c_p(u_r\frac{\partial T}{\partial r}+\frac{u_z}{h}\frac{\partial T}{\partial \eta})-k_0(\frac{1}{h^2}\frac{\partial^2 T}{\partial \eta^2}+\frac{\partial^2 T}{\partial r^2}+\frac{1}{r}\frac{\partial T}{\partial r})+\frac{1}{h}\frac{\partial q_r}{\partial \eta}-\frac{\mu}{h^2}\left(\frac{\partial u_r}{\partial \eta}\right)^2=0, \tag{10}$$

where T is the temperature, c_p is the specific heat capacity and k_0 is the thermal conductivity of the fluid and q_r is the radiative heat flux. In view of the Rosseland approximation for radiation (Devi and Devi [29]), the radiative heat flux q_r is simplified as

$$q_r=-\frac{4\sigma}{3k^*}\frac{\partial T^4}{\partial z}, \tag{11}$$

where k^* and σ are the Stefan–Boltzmann constant and the mean absorption coefficient respectively. It is assumed that the temperature differences within the flow such that the term T^4 may be linearized. Hence, expanding T^4 in a Taylor series about T_2 and neglecting higher order terms, we get

$$T^4\cong 4{T_2}^3T-3{T_2}^4, \tag{12}$$

and therefore eq. (10) reduces to

$$\rho c_p(u_r\frac{\partial T}{\partial r}+\frac{u_z}{h}\frac{\partial T}{\partial \eta})-k_0(\frac{1}{h^2}\frac{\partial^2 T}{\partial \eta^2}+\frac{\partial^2 T}{\partial r^2}+\frac{1}{r}\frac{\partial T}{\partial r})+\frac{1}{h}\frac{\partial q_r}{\partial \eta}-\frac{\mu}{h^2}\left(\frac{\partial u_r}{\partial \eta}\right)^2=0, \tag{13}$$

where T is the temperature, c_p is the specific heat capacity and k_0 is the thermal conductivity of the fluid and q_r is the radiative heat flux.

The boundary conditions for the problem may be written as,

$$\left.\begin{aligned} &u_r(r,-h)=rE, u_r(r,h)=rE, u_z(r,-h)=0, u_z(r,h)=0,\\ &\nu_2(r,-h)=0, \nu_2(r,h)=0, T(r,-h)=T_1, T(r,h)=T_2, \end{aligned}\right] \tag{14}$$

where E is the parameter determining the stretching strength of both the upper & lower disks, having units of $\frac{1}{t}$. The partial differential eqs. (7) – (9) and (10) can be converted into ordinary ones by using the following similarity transformations,

$$\eta=\frac{z}{h},\ u_r=-\frac{rE}{2}f'(\eta),\ u_z=Ehf(\eta), \upsilon_2=-\frac{Er}{2h^2}g(\eta),\ \theta(\eta)=\frac{T-T_2}{T_1-T_2}, \tag{15}$$

where T_1 & T_2 are the temperatures at the lower & upper disks respectively. We see that the velocity field given in eq. (15) identically satisfies the continuity eq. (6) and hence represents a possible fluid motion. By using eq. (15) in eqs. (7) – (9) and (13), we get the following nonlinear ordinary differential equations in dimensionless form

$$(1+C_1)f''''-C_1g''-R\,ff'''-RM^2f''=0, \tag{16}$$

$$C_3 g'' + C_1(f'' - 2g) + RC_2\left(\frac{f'g}{2} - f\,g'\right) = 0, \tag{17}$$

$$\left(1+\frac{4}{3}Nr\right)\theta'' + \frac{1}{4}Pr\,Ec\,f''^2 - R\,Pr\,f\,\theta' = 0, \tag{18}$$

where $R = \frac{\rho E h^2}{\mu}$ is the stretching Reynolds number, $M = \sqrt{\frac{\sigma_e B_0^{\,2}}{\rho E}}$ is the magnetic parameter, $C_1 = \frac{\kappa}{\mu}$ is the vortex viscosity parameter, $C_2 = \frac{j}{h^2}$ is the microinertia density parameter, $C_3 = \frac{\gamma}{\mu h^2}$ is the spin gradient viscosity parameter, $Pr = \frac{\mu c_p}{k_0}$ is the Prandtl number, $Nr = \frac{4\sigma T_2^{\,3}}{k^* k_0}$ is the radiation parameter and $Ec = \frac{r^2 E^2}{c_p(T_1 - T_2)}$ is the Eckert number. Boundary conditions given in eq. (10) also get the form,

$$f(-1) = f(1) = 0,\ f'(-1) = -2,\ f'(1) = -2,\ g(-1) = 0,\ g(1) = 0,\ \theta(-1) = 1,\ \theta(1) = 0. \tag{19}$$

3. Computational procedure

We use quasi-linearization to construct the sequences of vectors $\{f^{(k)}\}, \{g^{(k)}\}$ and $\{\theta^{(k)}\}$, which converge to the numerical solutions of eqs. (16) - (18) respectively. To construct $\{f^{(k)}\}$ we linearize eq. (16), by retaining only the first order terms, as follows:

We set:

$$G(f, f', f'', f''', f'''') \equiv (1+C_1) f'''' - C_1 g'' - R\,ff''' - RM^2 f'',$$

and

$$G(f^{(k)}, f'^{(k)}, f''^{(k)}, f'''^{(k)}, f''''^{(k)}) + \left(f^{(k+1)} - f^{(k)}\right)\frac{\partial G}{\partial f^{(k)}} + \left(f'^{(k+1)} - f'^{(k)}\right)\frac{\partial G}{\partial f'^{(k)}} + \left(f''^{(k+1)} - f''^{(k)}\right)\frac{\partial G}{\partial f''^{(k)}} +$$

$$\left(f'''^{(k+1)} - f'''^{(k)}\right)\frac{\partial G}{\partial f'''^{(k)}} + \left(f''''^{(k+1)} - f''''^{(k)}\right)\frac{\partial G}{\partial f''''^{(k)}} = 0,$$

which simplifies to:

$$(1+C_1) f''''^{(k+1)} - R\,f'''^{(k+1)} f^{(k)} - RM^2 f''^{(k+1)} - Rf'''^{(k)} f^{(k+1)} = C_1 g''^{(k)} - Rf'''^{(k)} f^{(k)}. \tag{20}$$

Now eq. (20) gives a system of linear differential equations, with f^k being the numerical solution vector of the k^{th} equation. To solve the linear ODEs, we replace the derivatives with their central difference approximations, giving rise to the sequence $\{f^{(k)}\}$, generated by the following linear system

$$Bf^{(k+1)} = C \text{ with } B \equiv B_{n\times n}\left(f^{(k)}\right) \text{and } C \equiv C_{n\times 1}\left(f^{(k)}\right), \tag{21}$$

where *n* is the number of grid points. On the other hand, eqs. (17) - (18) are linear in g and θ respectively, and therefore, in order to generate the sequences $\{g^{(k)}\}$ and $\{\theta^{(k)}\}$, we write

$$C_3 g''^{(k+1)} + C_1\left(f''^{(k+1)} - 2g^{(k+1)}\right) + RC_2\left(\frac{f'^{(k+1)} g^{(k+1)}}{2} - g'^{(k+1)} f^{(k+1)}\right) = 0, \tag{22}$$

$$\left(1+\frac{4}{3}Nr\right)\theta''^{(k+1)} + \frac{1}{4}Pr\,Ec\,f''^{(k+1)2} - R\,Pr\,f^{(k+1)}\theta'^{(k+1)} = 0. \tag{23}$$

Importantly $f^{(k+1)}$ is considered to be known in the above equation and its derivatives are approximated by the central differences.

We outline the computational procedure as follows:

- Provide the initial guess $f^{(0)}, g^{(0)} \& \theta^{(0)}$, satisfying the boundary conditions given in eq. (19)
- Solve the linear system given by eq. (21) to find $f^{(1)}$
- Use $f^{(1)}$ to solve the linear system arising from the FD discritization of eqs. (22) - (23), to get $g^{(1)} \& \theta^{(1)}$.
- Take $f^{(1)}, g^{(1)} \& \theta^{(1)}$ as the new initial guesses & repeat the procedure to generate the sequences $\left\{f^{(k)}\right\}, \left\{g^{(k)}\right\} \& \left\{\theta^{(k)}\right\}$ which, respectively, converge to $f, g \& \theta$ (the numerical solutions of eqs. (16) - (18).
- The three sequences are generated until

$$\max\left\{\left\|f^{(k+1)}-f^{(k)}\right\|_{L_\infty}, \left\|g^{(k+1)}-g^{(k)}\right\|_{L_\infty}, \left\|\theta^{(k+1)}-\theta^{(k)}\right\|_{L_\infty}\right\} < 10^{-6}.$$

It is important to note that the coefficient matrix B in eq. (21) will be pentadiagonal & not diagonally dominant, and hence the iterative method (like SOR) may fail or work very poorly. Therefore, some direct method like LU factorization or Gaussian elimination with full pivoting (to ensure stability) may be employed. On the other hand, eqs. (22) - (23) will give rise to the diagonally dominant algebraic system when discretized using the central differences, which allows us to use the SOR method. Lastly, we may also improve the order of accuracy of the solution by using polynomial extrapolation scheme.

5. Results and discussion

In this section we present our findings in tabular and graphical forms together with the discussion and their interpretations. Our objective is to develop a better understanding of the effects of micropolar structure of fluids on flow and heat transfer characteristics. The parameters of the study are the magnetic parameter *M*, the Reynolds number R, the micropolar parameters C_1, C_2 and C_3, the Eckert number Ec, the radiation parameter *Nr* and the Prandtl number *Pr*.

Following Hayat and Nawaz [19] and Hayat *et al* [26], the skin friction C_f, the wall couple stress C_g, and the Nusselt number Nu at $z = h$ are

$$C_f = \frac{\tau_w}{\rho(u_w)^2} = \frac{(\mu+\kappa)}{\rho(rE)^2}\left(\frac{\partial u}{\partial z}+\frac{\partial w}{\partial r}\right)\Bigg|_{z=h} = -\frac{1}{2}\frac{(1+C_1)}{Re_r} f''(1),\ C_g = \frac{\gamma \left.\frac{\partial \upsilon_2}{\partial z}\right|_{z=h}}{\rho(u_w)^2} = \frac{\gamma \left.\frac{\partial \upsilon_2}{\partial z}\right|_{z=h}}{\rho(rE)^2} = \frac{1}{2}\frac{C_3}{Re_r} g'(1),$$

and

$$Nu = \frac{h\, q_w}{k\left(T_1 - T_2\right)} = -\frac{hk \left.\frac{\partial T}{\partial z}\right|_{z=h}}{k\left(T_1 - T_2\right)} = -\theta'\left(1\right),$$

where $Re_r = \dfrac{\rho E h r}{\mu}$ is the local Reynolds number.

We will study the effects of the parameters described above on $C_f Re_r, C_g Re_r$ and Nu, as well as on the velocity profiles $f\ (\eta), f'(\eta)$, the microrotation profile $g(\eta)$ and the temperature profile $\theta(\eta)$.

All the cases of the micropolar parameters in the present work are shown in tab. 1. In order to establish the validity of our numerical computations and to improve the order of accuracy of the solutions,

numerical results are computed for three grid sizes $h, \frac{h}{2} \& \frac{h}{4}$ and then Richardson extrapolation is used as presented in tab. 2. It also shows the convergence of our numerical results as the step size decreases.

Table 3 predicts that both the skin friction coefficient $C_f Re_r$ and the couple stress coefficient $C_g Re_r$, as well as the Nusselt number Nu increase as the stretching Reynolds number R increases. The increased stretching rate of the disks forces the fluid to move rapidly towards the disks, thus increasing both the shear and couple stresses. Moreover, the fluid is carrying away the heat from the flow region, resulting in increasing the temperature difference and hence the heat transfer rate.

Table 4 shows that the magnetic parameter increases both the skin friction and the couple stress coefficient while reducing the Nusselt number at the disks. From the mechanical point of view, the magnetic field exerts a friction like force, called the Lorentz force, which tends to drag the fluid towards the disks. This not only results in increasing the skin friction coefficient at the disks but also causes greater spinning of the micro fluid particles, and hence increases the couple stress coefficient as well. Furthermore, the frictional force tends to raise the fluid temperature and thus decreases the temperature difference between the fluid and the disks. Therefore, the heat transfer rate, which is directly proportional to the temperature difference, also decreases. The influence of the micropolar parameters C_1, C_2 and C_3 on the shear and the couple stresses is given in tab. 5. The first case corresponds to the Newtonian fluid whereas the remaining ones are taken arbitrarily to investigate their influence on the flow as chosen in the literature [28-31]. It may be concluded that the microplar structure of the fluid tends to increase the skin friction coefficient while causing the microrotation in the fluid which is responsible for the increase in the couple stress coefficient at the disks, as shown in the tab. 5. It is also clear from the table that the role of the micro fluid particles in increasing the heat transfer rate is not as pronounced as compared to its effect on the shear and couple stresses. It is due to the reason that micropolar parameters do not appear in the heat eq. (14) and therefore do not directly influence the heat transfer characteristics of the problem. An increase in the Prandtl number always results in increasing the Nusselt number at the disks as shown in tab. 6. An increase in Prandtl number means that the heat energy is taken away from the flow region so that the temperature difference between the fluid and the disks increases, which results in enhancing the heat transfer rate at the disks. It is clear from tab. 7 that the effect of the radiation number is to decrease the heat transfer rate at the disks whether we consider or ignore the effects of the viscous dissipation. Table 8 shows that the viscous dissipation may cause thermal reversal at the lower disk while increasing the Nusselt number at the upper one, thus decreasing the temperature of the fluid which in turn increases temperature difference between the fluid and the upper disk, and hence the heat transfer rate at the upper disk.

For Eq. (16), the error residual after k^{th} is denoted by $\mathrm{Re}(f^{(k)})$ and is defined as:

$$\mathrm{Re}\left(f^{(k)}\right) = (1+C_1) f^{(k)'''} - C_1 g^{(k)''} - R f^{(k)} f^{(k)'''} - RM^2 f^{(k)''}.$$

Figure 2 shows $\mathrm{Re}(f^{(k)})$ after three iterations of the above mentioned computational procedure on a grid with 101 points. It is interesting to see that the maximum value of the error residual has dropped to 10^{-5} within just three iterations, which reflects the efficiency of the numerical algorithm.

Now we present the graphical interpretation of our results. Streamlines for the present problem are given in fig. 3. It is obvious that the streamlines near the walls are very close to each other showing larger gradients of the stream function which, in turn, predicts greater fluid velocity closer to the disks. Figures 4-8 predict the influence of the stretching Reynolds number R for a typical value of the magnetic parameter, the micropolar parameters, the Eckert number, the Prandtl number and the radiation parameter. The stretching Reynolds number decreases the velocity as well as the microrotation distribution across the disks (figs. 4-6). Whether we consider the viscous dissipation effects or not, Reynolds number always tends to flatten the

temperature profiles almost in the middle of the two disks, thus developing an equi-temperature region. On the other hand, it discourages the thermal reversal near the lower disk, for the case $Ec \neq 0$. From figs. 9-12, it is clear that the effect of M on the velocity and microrotation distribution is similar to that of R. On the other hand, the external magnetic field decreases the thermal reversal by decreasing the temperature distribution across the disks. It is noted that the effect of the micropolar structure of the fluid on the velocity, microrotation and temperature profiles is opposite to that of the magnetic field. Thus, the external magnetic field tends to balance the effect of the micropolar parameters. Figure 13 shows that the viscous dissipation tends to eliminate the symmetry of the temperature profiles by raising them near the lower disks, thus causing the thermal reversal. Finally, the effect of the Prandtl number on the heat profiles is opposite to that of radiation parameter (figs. 14-15), both in the presence and absence of the viscous dissipation.

6. Conclusions

In this paper, we numerically study how the governing parameters affect the flow and heat transfer characteristics of the steady, laminar, incompressible of an electrically conducting micropolar fluid between two stretchable infinite disks. Following conclusions have been drawn:

Micropolar fluids exhibit significant rise in the skin friction coefficient at the disks compared to the Newtonian ones, which may be beneficial for many industrial processes (e.g., in flow and thermal control of polymeric processing). Viscous dissipation may cause thermal reversal near the lower disk while significantly raising the temperature profile, whereas the external magnetic field magnifies the thermal reversal but lowers the temperature distribution, away from the lower disk. The external magnetic field, in this way, supports the viscous dissipation near the lower disk but opposes it away from the disk. Therefore the combined effect of the external magnetic field and viscous dissipation may be taken care of while simulating the flow between the disks. The effect of the radiation number is to decrease the Nusselt number rate at the disks.

Nomenclature

r, z	Cylindrical coordinates, [m]
u, v, w	Velocity components, [ms^{-1}]
c_1	Vortex viscosity, [$kgm^{-1}s^{-1}$]
c_2	Spin gradient viscosity, [$kgms^{-1}$]
c_3	Microinertia density, [m^2]
R	Stretching Reynolds number, [-]
M	Magnetic parameter, [-]
Pr	Prandtl number, [-]
Nr	Radiation parameter, [-]
Ec	Eckert number, [-]
c_p	Specific heat, [m^2s^{-2}]
p	Pressure, [$kgm^{-1}s^{-2}$]
k_0	Thermal conductivity, [$kgms^{-3}K^{-1}$]
T	Temperature, [K]
T_1, T_2	Fixed temperatures of the lower and upper disks respectively, [K]

Greek Symbols

κ, γ	Viscosity coefficients
μ	Dynamic viscosity, [Nsm^{-2}]
ν	Kinematic viscosity, [m^2s^{-1}]
ρ	Density, [kgm^{-3}]
η	Similarity variable

Subscripts

1	Condition at the lower disk
2	Condition at the upper disk

Superscripts

‘	Differentiation w.r.t η

Table 1. Five cases of values of micropolar parameters C_1, C_2 & C_3

Case No.	C_1	C_2	C_3
1(Newtonian)	0	0	0
2	2	0.2	0.3
3	4	0.4	0.5
4	6	0.6	0.7
5	8	0.8	0.9

Table 2. Dimensionless temperature $\theta(\eta)$ on three grid sizes and extrapolated values for $R=50, M=1, C_1=2, C_2=0.4, C_3=0.2, Pr=0.5, Ec=0.2$

	$\theta(\eta)$			
η	1st grid	2nd grid	3rd grid	Extrapol. values
-0.6	0.611051	0.611063	0.611066	0.611067
-0.2	0.519907	0.519904	0.519904	0.519904
0	0.500000	0.500000	0.500000	0.500000
0.2	0.480093	0.480095	0.480096	0.480096
0.6	0.388949	0.388936	0.388933	0.388932

Table 3. The effect of stretching Reynolds number on $\mathrm{Re}_r C_f$, $\mathrm{Re}_r C_g$, Nu **for** $M=1, C_1=2, C_2=0.2, C_3=0.3, Pr=0.7, Nr=1, Ec=0.2$

R	$\mathrm{Re}_r C_f$	$\mathrm{Re}_r C_g$	Nu
0	7.7391	1.1584	0.6812
10	10.9395	1.2740	0.9039
20	13.7080	1.3347	1.0969
30	16.0791	1.3674	1.2691
40	18.1509	1.3852	1.4266

Table 4. The effect of magnetic parameter on $\mathrm{Re}_r C_f$, $\mathrm{Re}_r C_g$, Nu **with** $R=20, C_1=2, C_2=0.2, C_3=0.3, Pr=0.7, Nr=1, Ec=0.2$

M	$\mathrm{Re}_r C_f$	$\mathrm{Re}_r C_g$	Nu
0	10.5522	1.2595	1.1645
0.5	11.4483	1.2816	1.1413
1.0	13.7080	1.3347	1.0969
1.5	16.6320	1.3970	1.0616
2.0	19.8207	1.4560	1.0419

Table 5. The effect of micropolar parameters on $\mathrm{Re}_r C_f$, $\mathrm{Re}_r C_g$, Nu **with** $R=20, M=1, Pr=0.7, Nr=1, Ec=0.2$

Cases	$\mathrm{Re}_r C_f$	$\mathrm{Re}_r C_g$	Nu
1	7.3418	0	1.0369
2	13.7080	1.3347	1.0969
3	18.9298	2.4190	1.1429
4	23.8937	3.4572	1.1732
5	28.7612	4.4781	1.1944

Table 6. The effect of Prandtl number on Nu **with** $R=3, M=1, C_1=2, C_2=0.2, C_3=0.3, Nr=2$

Pr	$Ec=0.0$	$Ec=0.3$
	Nu	Nu
3	0.6777	1.5331
8	1.0189	4.1180
13	1.3757	8.8125
18	1.7133	18.3785
21	1.9004	29.0152

Table 7. The effect of radiation parameter on Nu **with** $R=20, M=1, C_1=2, C_2=0.2, C_3=0.3, Pr=0.7$

Nr	$Ec=0.3$	$Ec=0.3$
	Nu	Nu
0.0	1.4399	2.1557
0.1	1.3196	1.9109
0.5	1.0319	1.3822
3.0	0.6576	0.7575
10.0	0.5522	0.5856

Table 8. The effect of viscous dissipation on $\theta'(-1)$, Nu **with** $R=20, M=1, C_1=2, C_2=0.2, C_3=0.3, Pr=0.7, Nr=1.0$

Ec	$-\theta'(-1)$	Nu
0.0	0.864027	0.864027
0.3	0.514688	1.213367
0.6	0.165348	1.562707
0.9	-0.183992	1.912046
1.2	-0.533331	2.261386

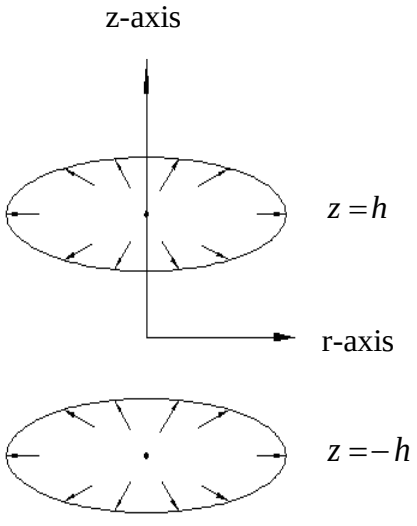

Figure 1. Physical Configuration

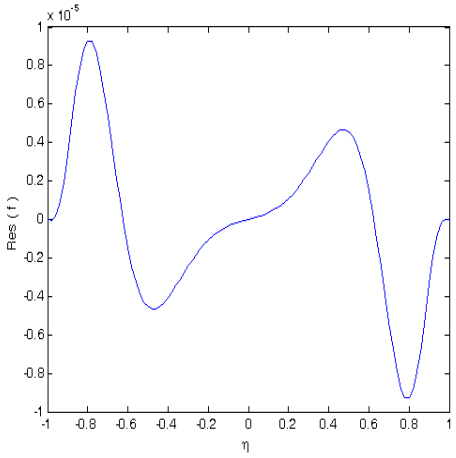

Figure 2. Error residual of $f(\eta)$ after three iterations

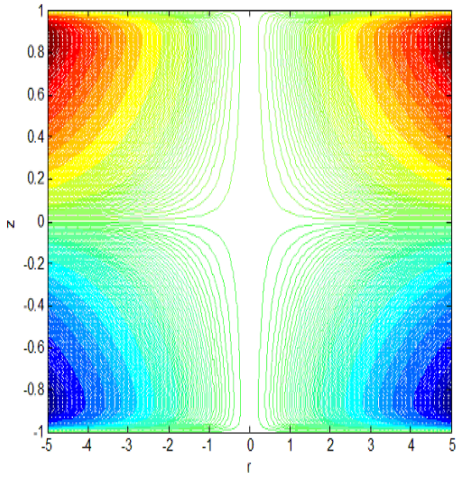

Figure 3. Streamlines for the problem.

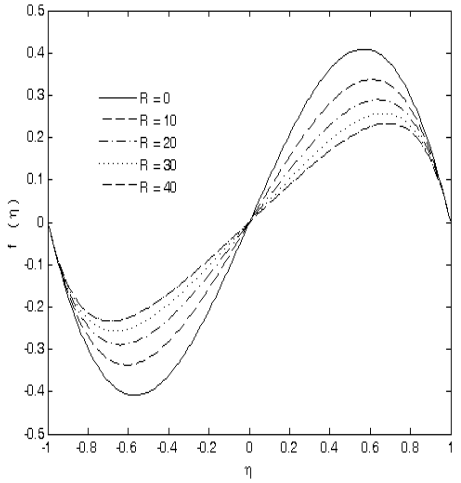

Figure 4. Variation of axial velocity for various R.

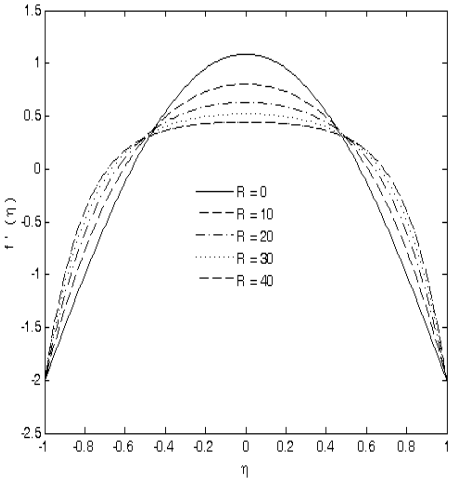

Figure 5. Variation of radial velocity for various R.

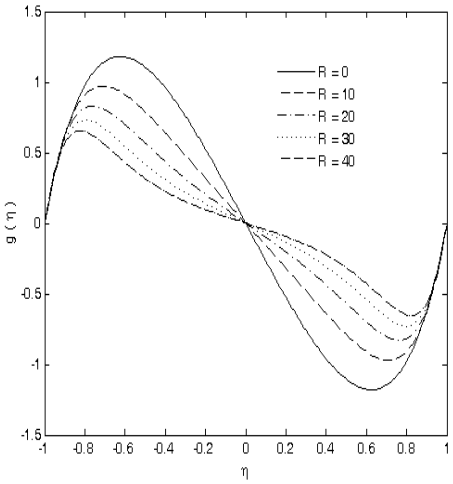

Figure 6. Variation of microrotation for various R.

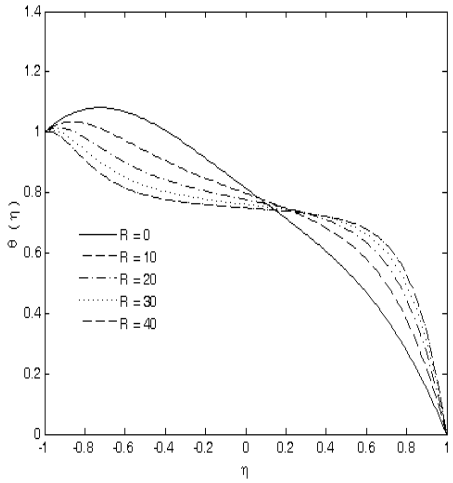

Figure 7. Variation of temperature for various R.

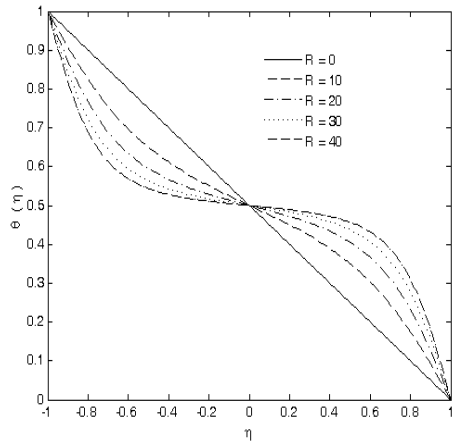

Figure 8. Variation of temperature for various R.

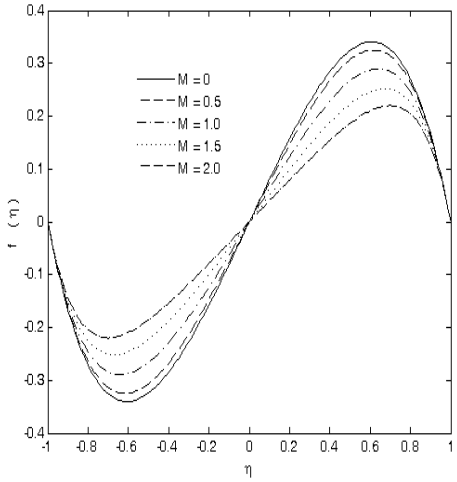

Figure 9. Axial velocity for various M.

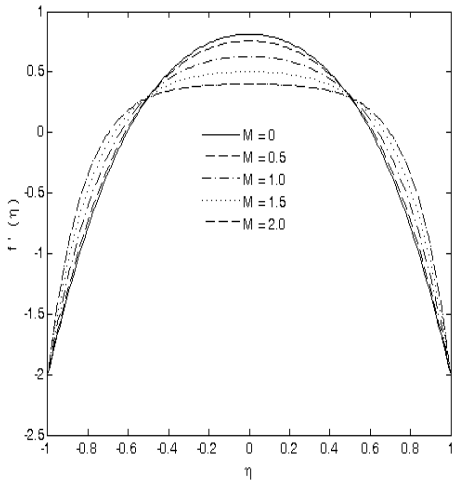

Figure 10. Radial velocity for various M.

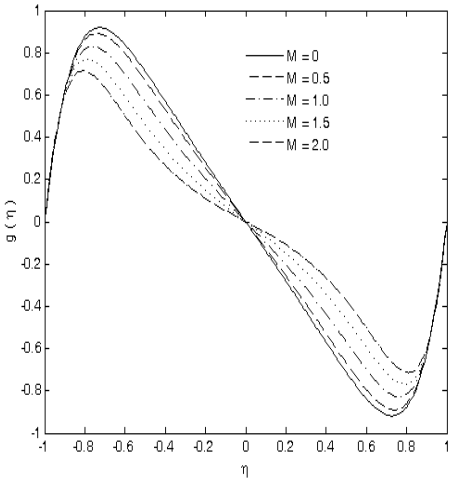

Figure 11. Microrotation for various M.

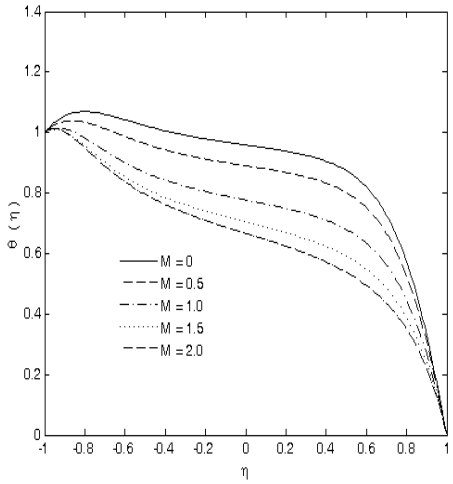

Figure 12. Temperature for various M.

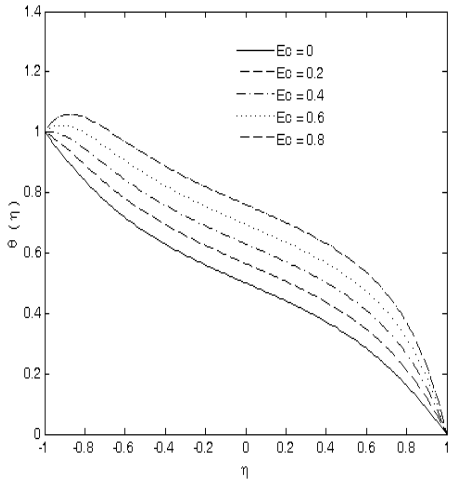

Figure 13. Temperature for various Ec.

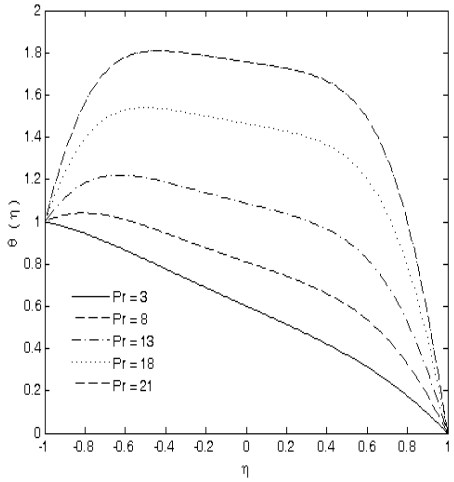

Figure 14. Variation of temperature for various *Pr*.

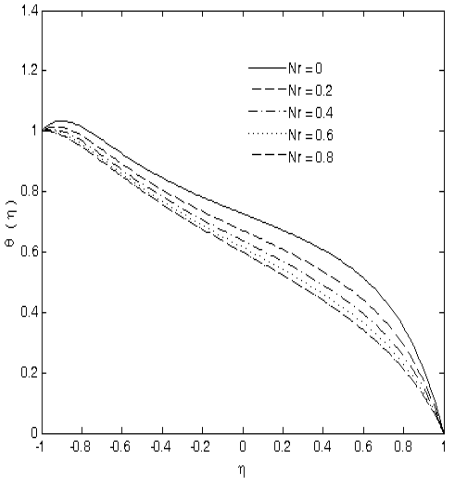

Figure 15. Variation of temperature for various *Nr*.

References

[1] Altan, T., *et al., Metal forming fundamentals and applications*, American Society of Metals., Metals Park, OH, 1979

[2] Fisher, E. G., *Extrusion of plastics*, Wiley., New York, 1976

[3] Tadmor, Z., Klein, I., *Engineering principles of plasticating extrusion: Polymer Science and engineering series*, Van Norstrand Reinhold., New York, 1970

[4] Singh, A., *et al.*, Investigation on inward flow between two stationery parallel disks, *Int. J. heat and fluid flow*, 20 (1999), pp. 395-401

[5] Fang, T., *et al.*, MHD and slip viscous flow over a stretching sheet, *Comm. Nonlinear Sci. Numer. Simulat*., 14 (2009), pp. 3731-3737

[6] Volkan, E. H., An approximate solution for flow between two disks rotating about distinct axes at different speeds, *Math. Problems in Eng*., (2007), pp. 1-16

[7] Ahmad, N., *et al.*, Boundary layer flow and heat transfer past a stretching plate with variable thermal conductivity, *Int. J. of non-linear Mech*., 45 (2010), pp. 306-309

[8] Yoon, M S., *et al.*, Flow and heat transfer over a rotating disk with surface roughness, *Int. J. Heat and Fluid Flow*, 28 (2007), pp. 262-267

[9] Robert A, *et al.*, Analytical solutions of a coupled nonlinear system arising in a flow between stretching disks, *Applied Mathematics and Computation*, 216 (2010), pp. 1513–1523

[10] Fang, T., Zhang, J., Flow between two stretchable disks- An exact solution of the Navier-Stokes equations, *International Communications in Heat and Mass Transfer*, 35 (2008), pp. 892–895

[11] Munawar, S., *et al.*, Effects of slip on flow between two stretchable disks using optimal homotopy analysis method, *Canadian Journal of Applied Sciences*, 1 (2011), pp. 50-68

[12] Turkyilmazoglu, M., MHD fluid flow and heat transfer due to a stretching rotating disk, *Journal of Thermal Sciences*, 51 (2012) pp. 195-201

[13] Turkyilmazoglu, M., Purely analytic solutions of magnetohydrodynamic swirling boundary layer flow over a porous rotating disk, *Computers and Fluids*, 39 (2010), pp. 793-799

[14] Attia, H. A., Steady flow over a rotating disk in porous medium with heat transfer, *Nonlinear*

analysis: Modelling and Control, 14 (2009), pp. 21–26

[15] Xinhui, S., *et al.*, Homotopy analysis method for the asymmetric laminar flow and heat transfer of viscous fluid between contracting rotating disks, *Applied mathematical modeling*, 36 (2012), pp. 1806-1820

[16] Hoyt, J. W., Fabula, A. G., *The effect of additives on fluid friction*, U. S. Naval Ordinance Test Station Report., 1964

[17] Eringen, A. C., Theory of Micropolar Fluids, *Journal of Mathematics and Mechanics*, 16 (1966), pp. 1-18

[18] Rashidi, M. M., *et al.*, Analytic approximate solutions for heat transfer of a micropolar fluid through a porous medium with radiation, *Communications in Nonlinear Science and Numerical Simulation*, 16 (2011), pp. 1874–1889

[19] Hayat, T., Nawaz, M., Effect of heat transfer on magnetohydrodynamic axisymmetric flow between two stretching sheets, *Zeitschrift für Naturforschung*, 65a (2010), pp. 961-968

[20] Takhar, H. S., *et al.*, Finite element solution of micropolar fluid flow and heat transfer between two porous discs, *International Journal of Engineering Science*, 38 (2000), pp. 1907-1922

[21] Takhar, H. S., *et al.*, Finite element solution of micropolar fluid flow from an enclosed rotating disk with suction and injection, *Journal of Engineering Science*, 39 (2001), pp. 913-927

[22] Rashidi, M. M., Keimanesh, M., Using Differential Transform Method and Padé Approximant for Solving MHD Flow in a Laminar Liquid Film from a Horizontal Stretching Surface, *Mathematical Problems in Engineering*, doi:10.1155/2010/491319

[23] Rashidi, M. M., *et al.*, Investigation of Entropy Generation in MHD and Slip Flow over a Rotating Porous Disk with Variable Properties, *International Journal of Heat and Mass Transfer*, 70 (2014), pp. 892–917

[24] Rashidi, M. M., Erfani, E., Analytical Method for Solving Steady MHD Convective and Slip Flow due to a Rotating Disk with Viscous Dissipation and Ohmic Heating, *Engineering Computations*, 29, (2012), pp. 562-579

[25] Shercliff, J. A., *A text book of magnetohydrodynamics*, Pergamon Press Oxford, 1965

[26] Hayat, T., *et al.*, Axisymmetric magnetohydrodynamic flow of a micropolar fluid between unsteady stretching surfaces, *Applied Mathematics and Mechanics*, 32 (2011), pp. 361-374

[27] Devi, S. P. A., Devi, R. U., On hydromagnetic flow due to a rotating disk with radiation effects, *Nonlinear Analysis: Mod. Cont*., 16 (2011), pp. 17-29

[28] Ashraf, M., *et al.*, Numerical investigations of asymmetric flow of a micropolar fluid between two porous disks, *Acta Mechanica Sinica*, 25 (2009), pp. 787-794

[29] Ashraf, M., *et al.*, Numerical study of asymmetric laminar flow of micropolar fluids in a porous channel, Computers and Fluids 38 (2009), 1895-1902

[30] Ashraf, M., Batool, K., MHD flow of a micropolar fluid over a stretching disk, *J. Theo. Appl. Mech.*, 51 (2013), 25-38

[31] Ali, K., *et al.*, Numerical simulation of MHD micropolar fluid flow and heat transfer in a channel with shrinking walls, *Canadian Journal of Physics*, 9 (2014), pp. 987-996